Giant coercivity of dense nanostructured spark plasma sintered barium hexaferrite

F. Mazaleyrat,[1, a)] A. Pasko,[1] A. Bartok,[1, b)] and M. LoBue[1]
SATIE, ENS Cachan, CNRS, Universud, 61 av President Wilson, F-94235, Cachan, France

(Dated: 18 January 2013)

Enhencement of the coercivity of ferrite magnets in order to make them true hard magnets – i.e. to get a coercive field higher than the residual magnetization– is still a very important issue due to the limited ressource in rare-earth. Thus, an alternative can be found in making very fine grain ferrite magnets but it is usually impossible to get small grains and dense material together. In this paper, it is shown that the spark plasma sintering method (SPS) is able to produce close to 80% dense material with crystallites smaller than 100 nm. The as prepared bulk sintered anisotropic magnets exibits coercive field of 0.5 T which is close to 60% of the theoretical limit and only few % below that of loose nano-powders. As a result, the magnets behave nearly ideally (-1.18 slope in the BH plane second quandrant) and the energy product reaches 8.8 kJm^{-3}, the highest value achieved in isotropic ferrite magnet to our knowledge.

PACS numbers: 75.50.Tt, 75.50.Ww, 75.50.Gg, 75.75.Cd,

I. INTRODUCTION

In the last years, much efforts have been devoted to the enhancement of the coercivity of hexagonal M-ferrites. The most fructuous results have been obtained by substitution of La and Co in strontium ferrite according to the formula $Sr_{1-x}La_xFe_{12-y}Co_yO_{19}$[1]. A very good compromize have been found for equi-molar La and Co compound with $x = y = 0.2$. Under optimal processing and sintering conditions, anisotropic magnets have been obtained with a very good rectangularity and an intrinsic coercivity as high as 334 kAm^{-1}(viz. $\mu_0 H_{CJ} = 0.42$ T) which represents a 20% improvement compared to regular anisotropic Sr magnets. This very good result, however, has to be compared with the anisotropy field $\mu_0 H_K = 2.27$ T of this compound, showing that, alltogether, the coercivity is only a fifth of the anisotropy field. This effect, known as Brown's paradox, is related to magnetic domain structure. On the other hand, a strong enhencement of the coercivity can be obtained by reducing the grain size below the single domain limit as it was proposed by Néel in 1942 (published ony after World War 2[2,3]). According to this theory –usually referred under the name of Stoner & Wohlfarth[4]– the upper limit of the coercivity is H_K for perfectly oriented and $0.48 \times H_K$ for an assembly of non-interacting uniaxial particles with isotropic distribution of easy axes. Several authors have succeed to produce $BaFe_{12}O_{19}$ nanoparticles by soft chemical route and they have found coercivities as high as 0.58 T for a mean grain size about 100 nm[5,6]. As the anisotropy field is 1.7 T, the theoretical value for an isotropic magnet is 0.82 T, so that they reached 70% of the upper limit, showing how promising should be this route. There is however a big drawback with this approach: these results have been obtained with loose powders only, whereas in practice, it is necessary to supply solid magnets. On the one hand, embeding in resin can keep this high coercivity but reduce dramatically the residual induction (due to dilution effect) in such a way that the energy product is not improved. On the other hand, sintering produce grain growth and the coercivity drops down to about 0.2 T. In this paper, we are showing that, starting from hexaferrite nanopowder, Spark Plasma Sintering (SPS) allows to produce nonostructured Ba-ferrite with a density close to 90% with almost no reduction in coercivity by opposition to SPS synthesis of nanosize Ba-ferrite in a single step[7,8].

II. EXPERIMENTAL DETAILS

Barium hexaferrite powders have been prepared by a sol-gel citrate precursor method[9–11]. High purity iron(III) nitrate, barium hydroxide and citric acid were used as starting materials with the molar ratio of citrate to metal ions 2:1. Iron(III) nitrate was dissolved in deionized water and quantitatively precipitated with excess of ammonia solution as iron(III) hydroxide. The precipitate was filtered and washed with water until neutrality. Then the obtained iron(III) hydroxide was dissolved in a vigorously stirred citric acid solution at 60-70°C. Barium hydroxide was added according to the desired composition. Polycondensation reaction with ethylene glycol to prevent segregation[9] was not used. Instead, pH value of the solution was adjusted to 6 for better chelation of metal ions[11]. Water was slowly evaporated at 80-90°C with continuing stirring until a highly viscous residue is formed. The gel was dried at 150-170°C and heat treated at 450°C for 2 hours for total elimination of organic matter. Finally, the inorganic precursor with homogeneous cationic distribution was calcined at 900°C for 2 hours

[a)] Electronic mail: mazaleyrat@satie.ens-cachan.fr; http://www.satie.ens-cachan.fr
[b)] Presently at LGEP, Universite Paris Sud, Orsay.

Sample	Sintering	Lattice constants			Cr. size	Density	Hysteresis parameters		
Ref.	time (min)	a (nm)	c (nm)	v (nm^3)	D (nm)	(%)	m_S(Am^{2}kg^{-1})	m_R/m_S	$\mu_0 H_C$(T)
Lit*	single cryst.	0.58920	2.31830	0.69699	–	100			
Com†	coarse grain	0.58928	2.32010	0.69772	>1000	>95	62	0.51	0.26
CP	as calcinated	0.58946	2.32185	0.69867	60	–	55	0.51	0.56
SPS1	0	0.58878	2.32378	0.69764	70	76	66	0.57	0.51
SPS3	13	0.58858	2.32224	0.69670	84	88	66	0.57	0.49
SPS4	20	0.58892	2.32259	0.69761	77	86	62	0.58	0.49

TABLE I. Structural and magnetic parameters of calcinated powder and SPS samples. Accuracy is ±5 nm for grain size (from XRD) and ±1% for density. *Litterature values are given for reference; †refers to commercial magnet.

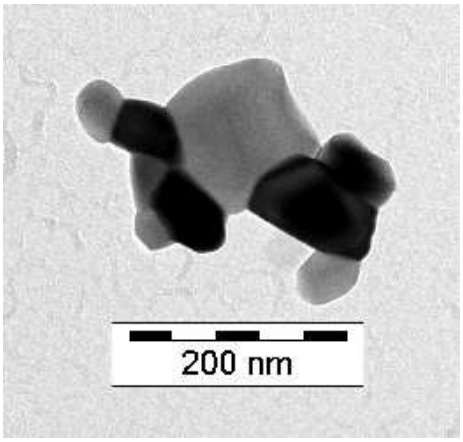

FIG. 1. Typical hexaferrite particle as received after clacination

with heating/cooling rate 200 K/hour to synthesize the barium hexaferrite phase. The calcination temperature have been chosen high enough to allow complete formation of the M phase and low enough to prevent grain growth. A representative TEM image of grain size and morphology is given in Fig.1. Details of this optimization procedure will be given in a forthcoming paper.

The samples have been sintered in a Sumitomo Dr Sinter spark plasma sintering (SPS) machine under a pressure of 50 MPa and neutral atmosphere in a graphite die. The heating rate was 160 Kmin^{-1}, up to 800°C. This temperature was kept for a duration between 0 and 20 min and then cooled at a rate of 200 K.min^{-1}.

XRD diffractograms have been recorded using a PANalytical X'Pert Pro equiped with a linear detector and the analysis of spectra was conducted with the Rietveld based software MAUD[12]. The morphology of sinterd sample was obsvered with a Hitachi SEM. Density was mesured using standart Archimedes method and the hysteresis loops where recorded at room temperature using a LakeShore vibrating sample magnetometer with a maximum field of 2 T.

III. RESULTS AND DISCUSSION

X-ray diffractogram of the powder after calcination shows all characteristic peaks of M-type hexaferrite (magnetoplumbite) with relatively broad shape. The lattice parameters are very close to those of literature reference samples and the average grain size was found to be about 60 nm (see Table I). This value obtained by fitting diffractograms with MAUD is confirmed by TEM (see Fig.1). Although some particles are bigger than 100 nm, most of then remains close to 50 nm. A slight decrease in the a axis paramer has been observed together with a increase of the c axis parameter upon sintering but it doesn't seem to be significant as the unit cell volume is almost constant. If this variation could be considered as significant, one would attribute it to internal stresses produced by the sintering process under uniaxial pressure. As expected with the SPS process, the average crystallite size is not much enhanced even after 20 min compared to the calcinated powder. This effect is related to the high speed of the process which allows atomic short range diffusion (involved in sintering process) but not long range diffusion (involved in grain growth process). In contrast, the density changes appreciably with time as it has been observed with most of materials sintered by SPS. A non negligible porosity remains after sintering as it is also seen in the SEM picture in Fig. 2. Only the sample SPS4 is shown but others exhibits very similar features. From these pictures, it is concluded that the material is composed of approximatively 1 µm grains composed of 70-80 nm crystallites with ∼500 nm node pores.

The hysteresis loops of the different samples are shown in Fig. 3. Comparison with conventional coarse-grain sample (commercial) immediatly shows the interest of reducing the grain size down to nm range: the sample measured after calcination in the form of loose powder exhibits a coercive field of 0.56 T, which is twice that of the coarse grain counterpart. In comparison with the theoretical field for an anisotropic magnet, this value is 70%, very close to results obtained by others[5,6]. The rectangularity of the loop is very close to 50% as expected from Néel calculations for a uniform distribution of easy axes. After SPS sintering, the density is already high, even for a very short heating-cooling cycle. A marked

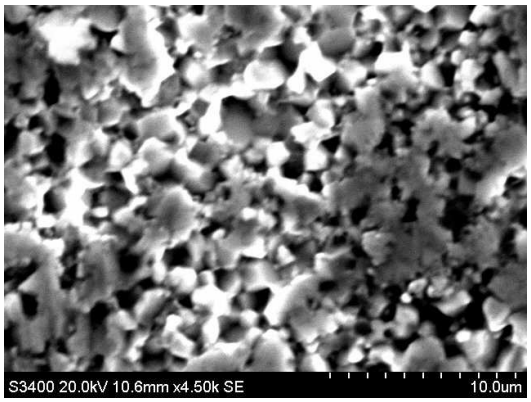

FIG. 2. SEM picture of sample SPS4

increase in saturation magnetization is observed, probably due to uncomplete transformation of the precursors during calcination. However, samples sintered for 0 to 13 min, still have sensitively higher value than the coarse grain sample, and drop to the same value for longer treatment time. This effect is probably due to an excess in oxygen gradually released due to the slightly reducing conditions.

The most stricking effect of SPS processing is the high value of the coercivity. Indeed, sintering reduces the coercive field, by only several tens of mT, so that coercivity values remain very close to 0.5 T for all SPS samples. This feature is due to the fact the crystallite size remains unchanged clearly under 100 nm, much below the single domain limit, $D_{SD} = 36\mu_0\sqrt{AK_1}/J_S^2 = 235\,\mathrm{nm}$ given after Kittel formula, where $K_1 = 338\,\mathrm{kJm^{-3}}$, $A = 5\,\mathrm{pJm^{-1}}$ and $J_S = 0.5\,\mathrm{T}$. As a consequence, nucleation of domain walls is impossible and the magnetization reversal should be processed by rotation. Although it is still far from the theoretical limit for isotropic magnets $0.48H_K \approx 0.85\,\mathrm{T}$ the coercivity is doubled compared to regular isotropic ferrite magnets. This feature is very important in applications, since it considerably improves the resistance upon demagnetization. From pratical point of view the characteristic in the BH plane is more relevant. Computation of the BH loop $B = \mu_0(\sigma\rho\delta + H)$, with σ the specific magnetization, ρ the bulk specific mass and δ the relative density, yields for the extrinsic coercivity $\mu_0 H_{CB} = 0.2\,\mathrm{T}$, the remnant induction $B_R = 0.23\,\mathrm{T}$ and the energy product $(BH)_{max} = 8.9\,\mathrm{kJm^3}$ compared with 0.15 T, 0.22 T and $7\,\mathrm{kJm^3}$ respectively for regualar sample.

IV. CONCLUSION

It has been demonstrated that SPS technique is an efficient and powerful tool for the sintering of nanostructured isotropic ferrite magnets as the coercivity of the powder can be obtained in dense samples. The energy product have been improved by 30% and the hardness

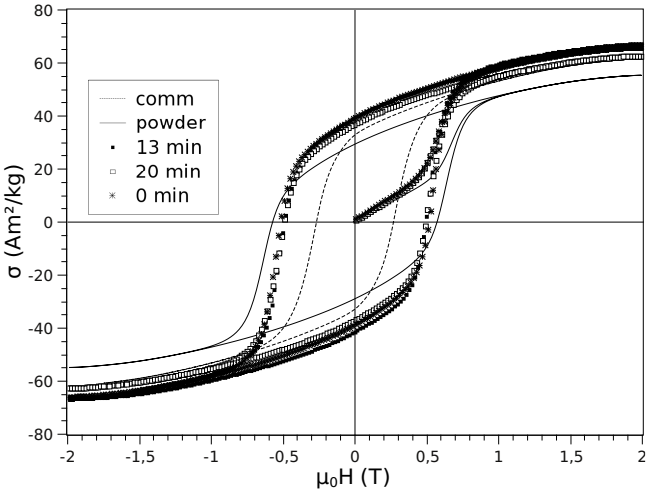

FIG. 3. Hysteresis (specic magnetization as a function of applied induction field) loops of commercial, as-calcinated and SPS sintered samples.

against demagnetization by a factor 2. In addition low temperature sintering meets the requirement of LTCC technology with no need of glass addition[13].

[1] P. Tenaud, A. Morel, F. Kools, J. Le Breton, and L. Lechevallier, J. Alloys & Compounds **370**, 331 (2004).
[2] L. Néel, Comptes Rendus. Acad. Sci. **224**, 94 (1947).
[3] L. Néel, Comptes Rendus.Acad.Sci. Paris **224**, 1550 (1947).
[4] E. Stoner and E. Wohlfarth, Trans. Roy. Soc. **A 240**, 599 (1948).
[5] Q. Pankhurst, G. Thompson, D. Dickson, and V. Sankaranarayanan, J. Magn. Magn. Mat. **155**, 104 (1996).
[6] W. Zhong, W. Ding, N. Zhang, Y. Du, Q. Yan, and J. Hong, J. Magn. Magn. Mat. **168**, 196 (1997).
[7] W. Zhao, Q. Zhang, X. Tang, H. Cheng, and P. Zhai, J. Appl. Phys. **99**, 08E909 (2006).
[8] W. Zhao, P. Wei, X. Wu, W. Wang, and Q. Zhang, Scripta materialia **59**, 282 (2008).
[9] F. Licci and T. Besagni, IEEE Trans. Magn. **20**, 1639 (1984).
[10] A. Srivastava, P. Singh, and M. Gupta, J.Mat. Science **22**, 1489 (1987).
[11] H. Yu and P. Liu, Journal of Alloys and Compounds **416**, 222 (2006).
[12] L. Luterotti, "Materails analysis using diffraction," Tech. Rep. (Universita di Trento, Italia, http://www.ing.unitn.it/ luttero/maud/index.html, 2003).
[13] Y. Liu, Y. Li, H. Zhang, D. Chen, and Q. Wen, J. Appl. Phys. **107**, 09A507 (2010).

ACKNOWLEDGMENTS

This work was partly supported by the EC FP7 project SSEEC under grant number NMP-SL-2008-214864. A.B. greatly aknowledge ENS Cachan for a 6 month scolarship in the frame of international scolarship program 2008/2009.

P. Audebert, Pr at ENS Cachan Chemical department PPSM-CNRS is greatly acknowledged for his advices in sol-gel production.